First-principles investigation on potential profile induced in graphene by surface and edge metal contacts

Takahisa Ohno*, Nobuo Tajima, and Jun Nara

Research Center for Materials Nanoarchitectonics (MANA),

National Institute for Materials Science (NIMS),

1-1 Namiki, Tsukuba, Ibaraki 305-0044, Japan

*E-mail: ohno.takahisa@nims.go.jp

Abstract

To utilize graphene as an electronic device graphene has to be brought into contact with a metal electrode and the metal contact has a significant impact on the characteristics of the device. We have investigated the potential profile induced in graphene layer by metal contacts, which describes how charges are redistributed between metal and graphene in order to eliminate the difference in work function between them, by using first-principles calculations. It is found that the potential profiles are much different between surface and edge contact metal/graphene junctions. For surface contacts the potential profile is significantly influenced by Pauli exclusion interactions and bond formation between metal and graphene. On the other hand, the edge contacts lack Pauli exclusion interactions and the non-graphene-like metallic states of C atoms near the metal edges, which are induced by bond formation, are suggested to have a major effect on eliminating the work function difference.

1. Introduction

Graphene exhibits outstanding properties[1,2] such as extremely high mobility[3] and it has drawn a great deal of attention as a promising materiel for future electric devices including field effect transistors,[4] photo-detectors[5,6] and so on. In order to make use of graphene as an electric device it is needed to bring into contact with a metal electrode. The metal/graphene junction has a significant impact on device properties, so understanding the properties of metal junction has important technological implications.

The junction geometries between metals and graphene can be divided into two main classes: surface contact and edge contact.[7,8] In the case of surface contact the graphene layer is deposited on the metal, whereas for the edge contact the graphene contacts with the metal at its edges. The edge-contact junctions exhibit remarkably lower contact resistance than the conventional surface-contact junctions due to the short bonding distances,[9,10] and are expected to offer new design possibilities for graphene devices.[7]

When a graphene comes into contact with a metal to form a metal/graphene junction, charge redistribution occurs between the metal and graphene due to the difference in work function (WF) between the two materials. The charge redistribution leads to graphene doping and generates a potential profile within the graphene, which significantly influences the electronic properties of graphene junction. The two-dimensional surface contact and the one-dimensional edge contact are supposed to exhibit different junction properties, especially those near the contact area. As for the surface contact, a number of experimental[11-13] and theoretical[14,15] studies have been conducted on graphene adsorbed on metal surfaces, and the potential profiles induced by contact with metals such as Al[16] and Ti[17] have also been studied using first-principles calculations. Compared to the surface contact, the junction properties of the edge contact are not well understood and the potential profiles has not been reported yet. In order to apply the edge contact to devices, it is necessary to understand their junction properties. In this paper, we theoretically investigate the electronic properties of the edge-contact metal/graphene junctions as well as the surface-contact junctions, and compare those potential profiles induced in graphene by metal contact.

2. Computational methods

The potential profile in the graphene junction can be expressed by the Fermi level shift with respect to the Dirac point, as long as the graphene-like band structure remains. We estimate the shift of the Fermi level (ΔE_F) along the graphene layer, which is called as the potential profile, by using the average electrostatic potential (V_{core}) at the core of C atom, following the method of potential profile

lineup[18,19] as follows,

$$\Delta E_F(r) = E_{Dirac}^{junc}(r) - E_F^{junc} = \left(E_{Dirac}^{junc}(r) - eV_{core}^{junc}(r)\right) - \left(E_F^{junc} - eV_{core}^{junc}(r)\right)$$
$$= \left(E_{Dirac}^{graphene} - eV_{core}^{graphene}\right) - \left(E_F^{junc} - eV_{core}^{junc}(r)\right). \quad (1)$$

Here E_{Dirac} and E_F are, respectively, the Dirac point energy and the Fermi level energy, and the superscripts "junc" and "graphene" stand for the systems of metal-graphene junction and isolated graphene, respectively. Here we assume that the difference between the Dirac point energy and the average core potential of C atom is fixed in the metal-graphene junction and isolated graphene. The Fermi level shift determined in this way is linearly dependent to the average core potential of C atoms. Negative and positive ΔE_F correspond, respectively, to n-type and p-type doping. If the Dirac point level of the graphene layer does not shift when contacted with metal, ΔE_F is the difference in work function (WF) between the metal and the graphene.

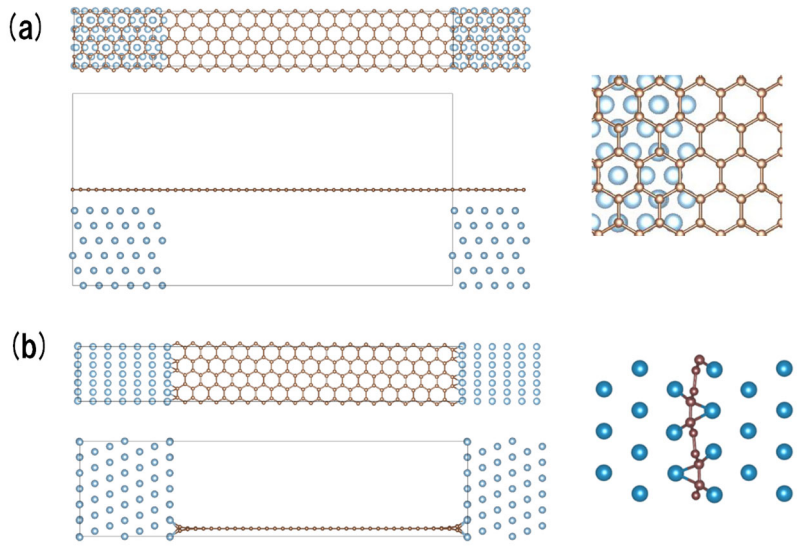

Fig.1. Schematics of (a) surface-contact and (b) edge-contact metal/graphene junctions. Their enlarged structures are also shown. The blue and brown spheres represent the metal and C atoms, respectively.

In this study we consider Al and Pd as typical metal electrodes. In case of surface contact, Al physisorbs on graphene while Pd chemisorbs. The metal/graphene junctions are modeled by the periodic supercell geometries, which are schematically shown in Fig.1. Graphene contacts with the metal (111) surfaces parallel and perpendicularly, respectively, for the surface and edge contact. For the surface contact, the unit cell is constructed from a slab of six metal layers with a graphene sheet

in contact with the topmost metal layer and a vacuum region of about 15 Å. For the edge contact, the metal surface is modeled by a slab of seven metal layers and both edges of the graphene sheet are perpendicularly bonded to the metal slab.[20] We fix the in-plane lattice constant of graphene to the optimized value of 2.46 Å, and adopt the same value for the lattice constants of the metals. The approximations made by this matching procedure are reasonable, because the lattice mismatch between graphene and metal surfaces is rather small: 0.5% for Al and 1.5% for Pd. In optimizing the geometry, the positions of the carbon atoms as well as those of the top two layers of the metal slab are allowed to be relaxed.

To study the atomic and electronic structures of the metal/graphene junctions, we employ Vienna ab initio simulation package (VASP)[21] wherein the projector-augmented wave (PAW) pseudopotentials[22] are taken and exchange–correlation energy is treated using the Perdew, Burke, and Ernzerhof gradient-corrected functional.[23] The van der Waals interaction correction is taken into account using the D2 approximation.[24] The wave functions are expanded into plane waves using a kinetic energy cutoff of 400 eV, and the Brillouin zone integrations are sampled by a k-mesh of 1x24x1 mesh. The geometries are optimized until the forces become less than 0.01 eV/Å.

3. Results and Discussion

3.1 Surface-contact junctions

We first investigate the graphene junction with surface-contact with metals. For the Al/graphene junction, the graphene is physically adsorbed on the Al surface in the contact region. The average separation between the topmost Al and the graphene layers is calculated to be 3.28 Å. and no chemical bonds are formed between them. The projected density of state (PDOS) on the C atom in the contact region is almost the same as that in the free-standing (FS) region with only just shifted, as shown in Fig.2 (b), which indicates that the graphene physically adsorbed on the Al surface maintains the intrinsic linear-dispersion electronic structure. The Fermi-level shift with respect to the Dirac point $\Delta E_F(z)$, that is the potential profile, along the junction is plotted in Fig.2 (a). The ΔE_F at the center of the contact region is –0.53 V, which means that the Dirac point is located 0.53 eV below the Fermi level and the graphene is doped n-type. In the FS region away from the Al surface, the ΔE_F gradually increases and remains negative. The results of the atomic structure and the potential profile are consistent with the previous theoretical calculations.[14-16]

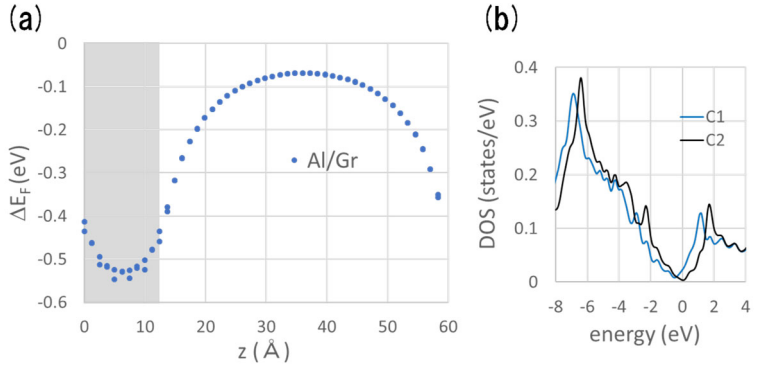

Fig.2. (a) Potential profile $\Delta E_F(z)$ along the surface-contact Al/graphene junction. (b) Projected density of states (PDOS) on the two C atoms: C1 is located just above the center of the Al contact, C 2 is at the center of the FS region. The Fermi level is set to be 0 eV. The metal contact area is indicated by shading.

For the surface-contact Pd/graphene junction the graphene is adsorbed on the Pd(111) surface with forming chemical bonds, different from the Al/graphene junction. The average separation between the topmost Pd and the graphene layers is 2.63 Å. Figure.3 (b) shows the PDOS on the C atoms near the edge of the Pd electrode. The C atoms bonded with Pd, such as the C1 atom with the bond length of 2.27 Å, lose to some extent the graphene-like electronic structures and have a metallic character with a finite density of states at the Fermi level. As leaving away from the edge of the Pd electrode the C atoms gradually recover the graphene-like PDOS, and the C4 and farther C atoms have the graphene-like electronic structure.

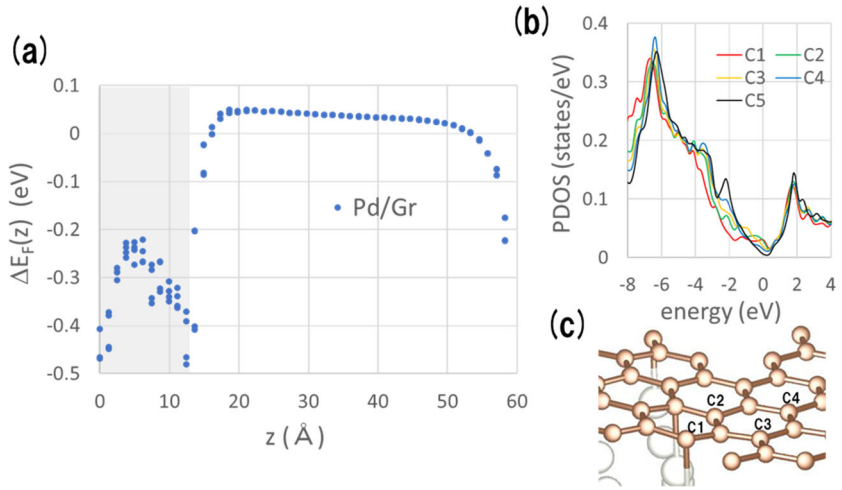

Fig.3. (a) Potential profile $\Delta E_F(z)$ along the surface-contact Pd/graphene junction. (b) Projected density of states (PDOS) on the C atoms numbered in (c) the geometry near the edge of the contact. The PDOS on the C5 atom at the center of the FS region is also shown. The Fermi level is set to be 0 eV. The metal contact area is indicated by shading.

The potential profile $\Delta E_F(z)$ along the junction is plotted in Fig.3 (a). This is the first report for the Pd/graphene junction using first-principles calculations, as far as we know. The ΔE_F are negative above the Pd electrode and become positive in the FS region.[25] The change of ΔE_F from negative to positive is consistent with the prediction from the numerical analysis based on the Thomas Fermi (TF) approximation.[26] It is noted that the negative values of ΔE_F of the C atoms above the Pd surface does not mean the n-type doping of graphene since these C atoms bonded with Pd do not have the graphene-like electronic structure, as explained above. The n/p transition of ΔE_F occurs very close to the Pd edge at the C4 atom, which has the graphene-like properties. Thus, almost all part of the graphene in the FS region acts as the p-doped graphene.

The Fermi level shift ΔE_F of the graphene adsorbed on metal surfaces have been extensively investigated.[14,15] Here, we examine the effect of metal contact on the potential profile $\Delta E_F(z)$ along the entire junction including the FS region. Figure 4 (a) shows the potential profile $\Delta E_F(z)$ in the surface-contact Al/graphene junction with varying the Al-graphene layer distance from 4.0 Å to the optimal 3.28 Å. At the Al-graphene layer distance of 4.0Å, the ΔE_F at the center of the contact region is –0.20 eV, which is nearly equal to the WF difference between Al (4.15 eV) and graphene (4.32 eV). When the graphene approaches the Al surface from 4.0 Å to 3.28 Å, the Pauli exclusion interaction takes effect between the electrons of Al and graphene, which induces the charge redistribution between Al and graphene and decreases the electrostatic potential at the graphene layer.[16] As a result, the ΔE_F of the C atom above the center of the Al surface decreases to –0.53 eV. The ΔE_F in the FS region also decreases as the ΔE_F of the contact region decreases.

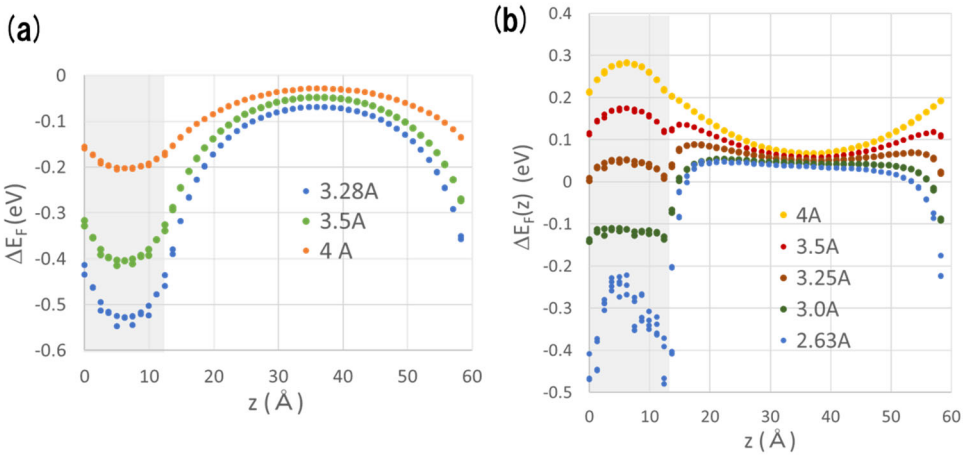

Fig.4. Potential profile $\Delta E_F(z)$ along the surface-contact (a) Al/graphene and (b) Pd/graphene junctions with varying the metal-graphene layer distance from 4.0 Å to their optimal distance of 3.28 Å and 2.63 Å. The metal contact area is indicated by shading.

The potential profile $\Delta E_F(z)$ in the surface-contact Pd/graphene junction with varying the Pd-graphene layer is shown in Fig.4 (b). When the distance between the graphene and Pd layers is 4.0 Å, the Fermi-level shift ΔE_F of the center of the contact region is 0.28 eV, which is much smaller than the WF difference between Pd (5.25 eV) and graphene (4.32 eV) of 0.93 eV, which may indicate that the Pauli exclusion interaction already takes effect at this layer distance. As the graphene layer approaches the Pd surface, the ΔE_F in the contact region decreases further due to the Pauli exclusion interaction, and when the graphene layer approaches 3.0 Å from the Pd surface the ΔE_F in the contact region takes negative values contrary to the WF difference. At the optimal Pd-graphene layer distance of 2.63 Å, some of the C atoms in the contact region form bonds with the Pd surface, which reduces further ΔE_F in the contact region. The C atom with a shorter Pd-C bond length tends to have a larger negative value of ΔE_F, thus the ΔE_F of the C atoms on the Pd surface has large variation in value depending on the Pd-C distances. As the ΔE_F in the contact region decreases significantly, the ΔE_F in the FS region also decreases to some extent. However, since there is no direct interaction between the electrons of Pd and graphene in the FS region, the ΔE_F takes a positive value in almost all the FS region, reflecting the difference in WF. In this way, the potential profile ΔE_F of the surface contact metal/graphene junction is strongly affected by the Pauli exclusion interaction and the bond formation between metal and graphene.

3.2 Edge-contact junctions

Different from the surface-contact metal/graphene junction having a wide two-dimensional contact region and a FS region, the edge-contact junction is composed of a one-dimensional contact region and a FS region and is expected to have different characteristics of potential profile. Hereafter, we investigate the edge-contact graphene junctions with Al and Pd. In the edge-contact metal/graphene junction, the graphene sheet is perpendicularly bonded to the metal (111) surface, as shown in Fig.1 (b), and Al and Pd form covalent bonds with graphene and the metal-C bond length ranges from 2.0 Å to 2.3 Å.

The potential profile $\Delta E_F(z)$ of the edge-contact Al/Graphene junction is shown in Fig.5 (a). Similar to the surface-contact shown in Fig.2 (a), the ΔE_F takes a negative value almost throughout the FS region except near the metal edge, but the negative values are considerably smaller compared with the surface-contact junction. For the Pd/Graphene junction shown in Fig.5 (b), the ΔE_F takes a positive value in the whole of the FS region and the values are much larger than the ΔE_F in the FS region of the surface contact shown in Fig.3 (a).

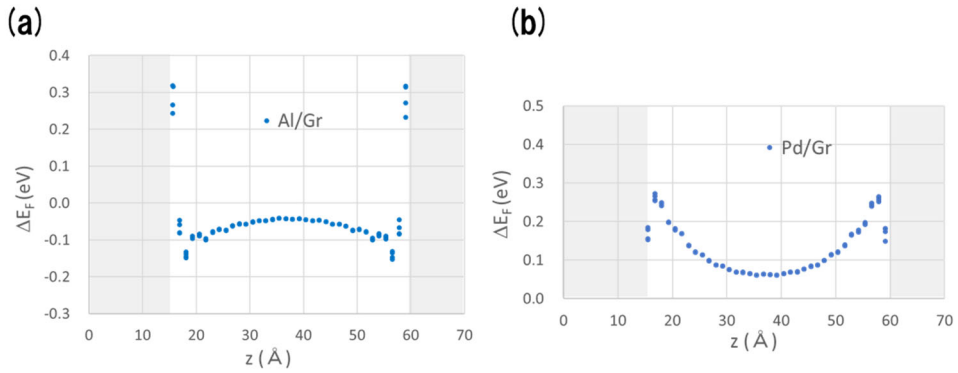

Fig.5. Potential profile $\Delta E_F(z)$ of the edge-contact Graphene junction with (a) Al and (b) Pd. The metal contact area is indicated by shading.

In this way, the potential profiles are much different between the surface and edge contacts. This is because the potential profile of the surface-contact junction is significantly affected by the Pauli exclusion interaction and the bond formation between the metal and graphene,[14] whereas the edge-contact junction lacks the Pauli exclusion interaction, which would decrease the electrostatic potential, that is ΔE_F, at the contact region. To elucidate the effect of bond formation at the edge contact, we consider the junction without metal-graphene bonds as shown in Fig. 6 (b), where all of the C atoms at the graphene edges are removed and the newly-formed edges are terminated by hydrogen atoms. The metal-hydrogen distance in the H-terminated contact is long enough not to form bonds.

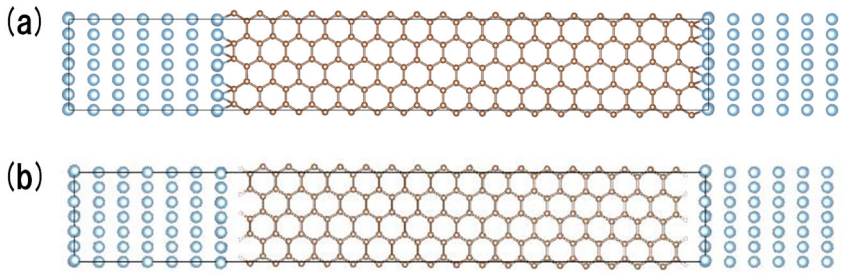

Fig.6. Schematics of (a) the edge-contact metal/graphene junction and (b) hydrogen-terminated edge-contact junction. Refer to the text for details.

Figures 7 (a) and (b) show the potential profiles $\Delta E_F(z)$ of the edge-contact Al/graphene and Pd/graphene junctions, respectively, where the graphene edge is bonded to metal or terminated with hydrogen. The potential profile ΔE_F of the metal-bonded edge-contact takes considerably smaller values than that of the H-terminated edge-contact. The potential profile induced in the graphene layer describes how charges are redistributed between metal and graphene in order to eliminate their WF difference. The smaller value of ΔE_F for the metal-bonded contact indicates that the WF difference is screened more effectively than the H-terminated contact. As shown in Fig. 8, for the edge-bonded

Pd/graphene junction the C atoms near the metal-bonded edge have a finite PDOS near the Fermi energy and exhibit non-graphene-like metallic electronic states, whereas the C atoms near the H-terminated edge have a much smaller PDOS. For the Al/graphene junction the C atoms near the metal-bonded edge have also metallic electronic states. These non-graphene-like metallic states induced by bonding with metals are considered to effectively contribute to eliminating the WF difference between metal and graphene and to decreasing ΔE_F in the FS region.

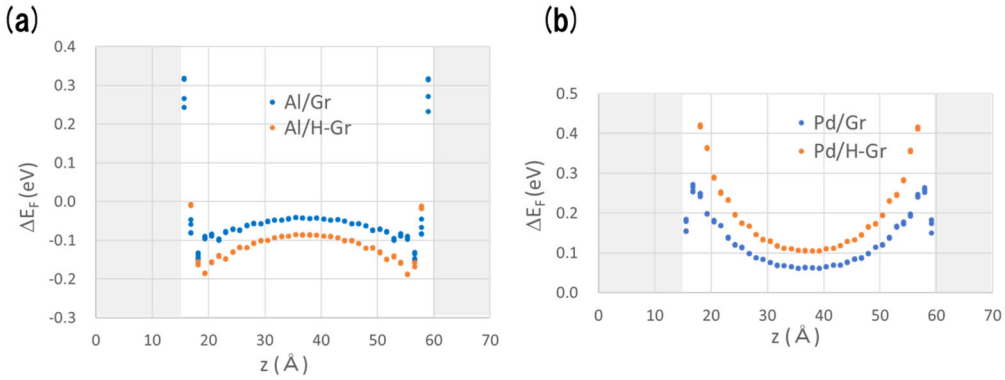

Fig.7. Potential profiles of the edge-contact (a) Al/graphene and (b) Pd/graphene junctions, where the graphene edge is bonded to metal or terminated with hydrogen. The metal contact area is indicated by shading.

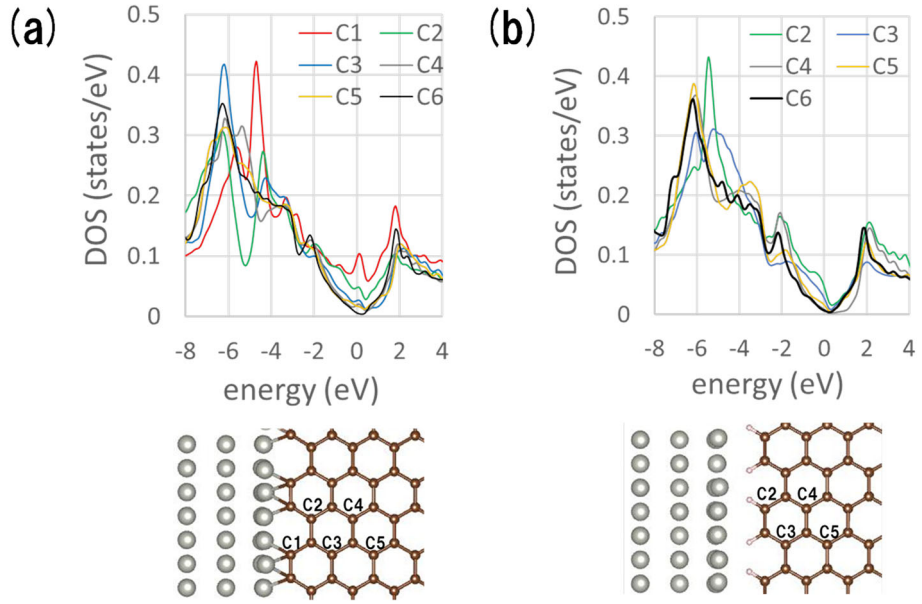

Fig.8. Projected density of states (PDOS) on the numbered C atoms near the graphene edge (a) bonded to Pd and (b) terminated with H, for the edge-contact Pd/graphene junction. The PDOS on the C6 atom at the center of the FS region is also shown. The Fermi level is set to be 0 eV.

The influence of metal-graphene bond formation at the edge contact depends on the atomistic contact geometry. So far, we have presented the results for the edge contacts where the armchair edge of graphene comes into contact with metal. Figures 9 (a) and (b) show the potential profiles $\Delta E_F(z)$ of the edge-contact Al/graphene and Pd/graphene junctions, respectively, comparing the two types of graphene edges: the armchair and zigzag edges. For the Pd/graphene junctions, the two types of edges have very similar potential profiles. In the case of Al/graphene junctions, however, the two edges exhibit quite different potential profiles: $\Delta E_F(z)$ is negative for the armchair edge, while is positive for the zigzag edge, which is contrary to the WF difference. Since the WF difference between Al and graphene is relatively small, the difference in the metal-graphene bonding geometry seems to result in the different potential profile. In this way, the metal-graphene bond formation at the edge contact is suggested to have a significant impact on the potential profile and doping properties.

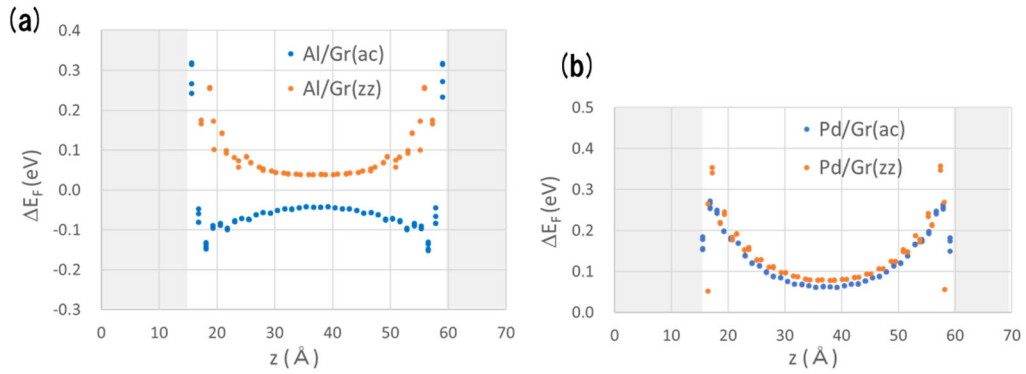

Fig.9. Potential profiles of the edge-contact (a) Al/graphene and (b) Pd/graphene junctions, comparing the two types of graphene edges: the armchair (ac) edge and the zigzag (zz) edge. The metal contact area is indicated by shading.

4. Conclusions

In this paper, we have theoretically investigated the electronic properties of the edge-contact metal/graphene junctions as well as surface-contact junctions. The potential profiles are much different between the surface and edge contacts. This is because the potential profile of the surface-contact junction is significantly affected by the Pauli exclusion interaction and the bond formation between the metal and graphene, whereas the edge-contact junction lacks the Pauli exclusion interaction. For the edge-contact junction, the non-graphene-like metallic states of C atoms near the metal edges, which are induced by bond formation, are considered to have a major effect on eliminating the work function difference between metal and graphene. The obtained understanding of the effects of the different types of metal contacts on the properties of metal/graphene junctions provides useful knowledge for application of graphene to devices.

Acknowledgements

This work was supported by Innovative Science and Technology Initiative for Security Grant Number JPJ004596, ATLA, Japan. The atomic structures shown in Figures 1, 3, 6, and 8 were drawn by using VESTA[27]. The calculations were performed by using the Numerical Materials Simulator of NIMS and the Earth Simulator (ES) of the Japan Agency for Marine-Earth Science and Technology (JAMSTEC).

References

1) M. Xu, T. Liang, M. Shi, and H. Chen, Chem. Rev. 113, 3766–3798 (2013).

2) A. K. Geim and I. V. Grigorieva, Nature 499, 419–425 (2013).

3) K. S. Novoselov, A. K. Geim, S. Morozov, D. Jiang, Y. Zhang, S. Dubonos, I. Grigorieva, and A. Firsov, Science 306, 666–669 (2004).

4) B.J. Kim, H. Jang, S.K. Lee, B.H. Hong, J.H. Ahn, and J.H. Cho, Nano Lett. 10, 3464–3466 (2010).

5) L. Ponomarenko, R. Gorbachev, G. Yu, D. Elias, R. Jalil, A. Patel, A. Mishchenko, A. Mayorov, C. Woods, and J. Wallbank, Nature 497, 594–597 (2013).

6) X. Cai et al. Nat. Nanotechnol. 9, 814–819 (2014).

7) L. Wang et al. Science 342, 614−617 (2013).

8) D. W. Yue, C. H. Ra, X. C. Liu, D. Y. Lee, and W. J. Yoo, Nanoscale 7, 825−831 (2015).

9) J.T. Smith, A.D. Franklin, D.B. Farmer, and C.D. Dimitrakopoulos, ACS Nano 7, 3661−3667 (2013).

10) S.M. Song, T.Y. Kim, O.J. Sul, W.C. Shin, and B.J. Cho, Appl. Phys. Lett. 104, 183506 (2016).

11) C. Oshima and A. Nagashima, J. Phys. Condens. Matter **9**, 1 (1997).

12) A. T. N'Diaye, S. Bleikamp, P. J. Feibelman, and T. Michely, Phys. Rev. Lett. **97**, 215501 (2006).

13) Y. S. Dedkov, A. M. Shikin, V. K. Adamchuk, S. L. Molodtsov, C. Laubschat, A. Bauer, and G. Kaindl, Phys. Rev. B **64**, 035405 (2001).

14) G. Giovannetti, P. A. Khomyakov, G. Brocks, V. M. Karpan, J. van den Brink, and P. J. Kelly, Phys. Rev. Lett. 101, 026803 (2008).

15) C. Gong, G. Lee, B. Shan, E.M. Vogel, R.M. Wallace, and K. Cho, J. Appl. Phys. 108, 123711 (2010).

16) S. Barraza-Lopez, M. Vanevic, M. Kindermann, and M.Y. Chou, Phys. Rev. Lett. 104, 076807 (2010).

17) S. Barraza-Lopez, M. Kindermann, and M.Y. Chou, Nano Lett. 12, 3424−3430 (2012).

18) W. Zhu and E. Kaxiras, Appl. Phys. Lett. 89, 243107 (2006).

19) Q. Ran, M. Gao, X. Guan, Y. Wang, and Z. Yu, Appl. Phys. Lett. 94, 103511 (2009).

20) We have adopted the atomic structures in which the graphene sheet is perpendicularly bonded to the metal (111) surface so as to intersect along the [1/2, 1/2, -1] direction. This structure is considered to maximize bond formation between C and metal atoms.

21) G. Kresse and J. Furthmuller, Phys. Rev. B 54, 11169−11186 (1996).

22) G. Kresse and D. Joubert, Phys. Rev. B 59, 1758−1775 (1999).

23) J.P. Perdew, K. Burke, and M. Ernzerhof, Phys. Rev. Lett. 77, 3865−3868 (1996).

24) S. Grimme, J. Comput. Chem. **27**, 1787 (2006).

25) The potential profile shows some degree of asymmetry since the atomic structures near the Pd edges are different to some extent between the left and right electrodes due to the different Pd-C bond formation.

26) P.A. Khomyakov, A.A. Starikov, G. Brocks, and P.J. Kelly, Phys. Rev. B 82, 115437 (2010).

27) K. Momma and F. Izumi, J. Appl. Crystallogr. 44, 1272 (2011).

Figure captions

Fig.1. Schematics of (a) surface-contact and (b) edge-contact metal/graphene junctions. Their enlarged structures are also shown. The blue and brown spheres represent the metal and C atoms, respectively.

Fig.2: (a) Potential profile $\Delta E_F(z)$ along the surface-contact Al/graphene junction, (b) projected density of states (PDOS) on the two C atoms: C1 is located just above the center of the Al contact, C 2 is at the center of the FS region. The Fermi level is set to be 0 eV. The metal contact area is indicated by shading.

Fig.3: (a) Potential profile $\Delta E_F(z)$ along the surface-contact Pd/graphene junction, (b) projected density of states (PDOS) on the C atoms numbered in (c) the geometry near the edge of the contact. The PDOS on the C5 atom at the center of the FS region is also shown. The Fermi level is set to be 0 eV. The metal contact area is indicated by shading.

Fig.4: Potential profile $\Delta E_F(z)$ along the surface-contact (a) Al/graphene and (b) Pd/graphene junctions with varying the metal-graphene layer distance from 4.0 Å to their optimal distance of 3.28 Å and 2.63 Å. The metal contact area is indicated by shading.

Fig.5: Potential profile $\Delta E_F(z)$ of the edge-contact graphene junction with (a) Al and (b) Pd. The metal contact area is indicated by shading.

Fig.6: Schematics of (a) the edge-contact metal/graphene junction and (b) hydrogen-terminated edge-contact junction. Refer to the text for details.

Fig.7: Potential profiles of the edge-contact (a) Al/graphene and (b) Pd/graphene junctions, where the graphene edge is bonded to metal or terminated with hydrogen. The metal contact area is indicated by shading.

Fig.8: Projected density of states (PDOS) on the numbered C atoms near the graphene edge (a) bonded to Pd and (b) terminated with H, for the edge-contact Pd/graphene junction. The PDOS on the C6 atom at the center of the FS region is also shown. The Fermi level is set to be 0 eV.

Fig.9. Potential profiles of the edge-contact (a) Al/graphene and (b) Pd/graphene junctions, comparing the two types of graphene edges: the armchair (ac) edge and the zigzag (zz) edge. The metal contact area is indicated by shading.

Figures

Figure 1

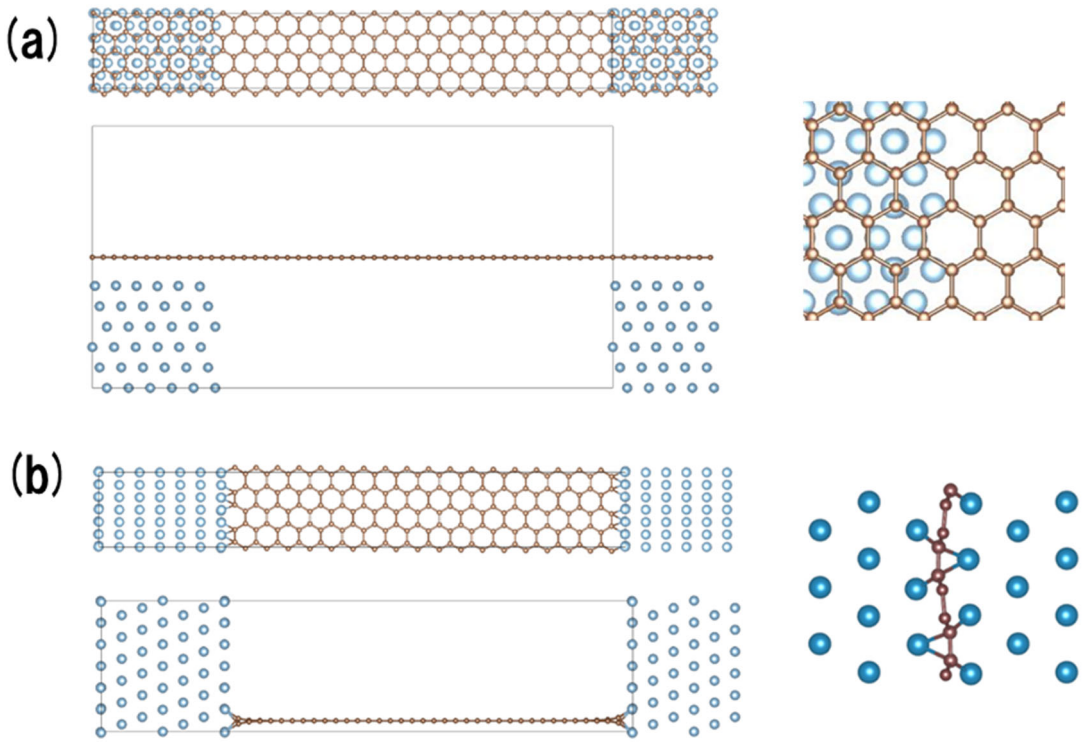

Figure 2

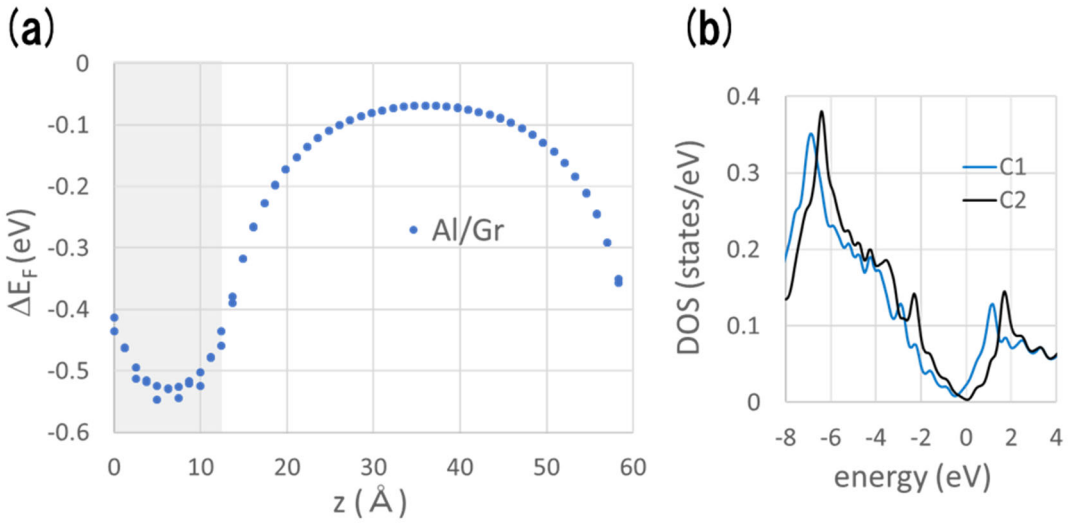
(a)
0
-0.1
-0.2
-0.3
-0.4
-0.5
-0.6
ΔE_F (eV)
Al/Gr
0
10
20
30
40
50
60
z (Å)
(b)
0.4
0.3
0.2
0.1
0
DOS (states/eV)
C1
C2
-8
-6
-4
-2
0
2
4
energy (eV)

Figure 3

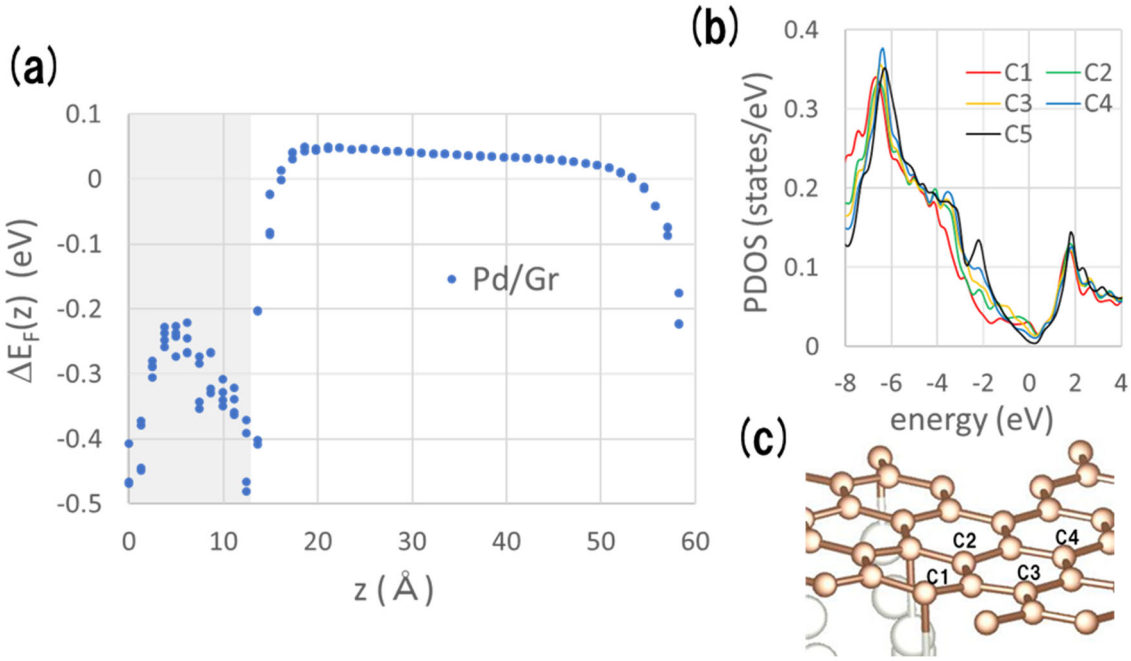
(a)
0.1
0
-0.1
-0.2
-0.3
-0.4
-0.5
ΔE_F(z) (eV)
Pd/Gr
0
10
20
30
40
50
60
z (Å)
(b)
0.4
0.3
0.2
0.1
0
PDOS (states/eV)
C1
C2
C3
C4
C5
-8
-6
-4
-2
0
2
4
energy (eV)
(c)
C2
C4
C1
C3

Figure 4

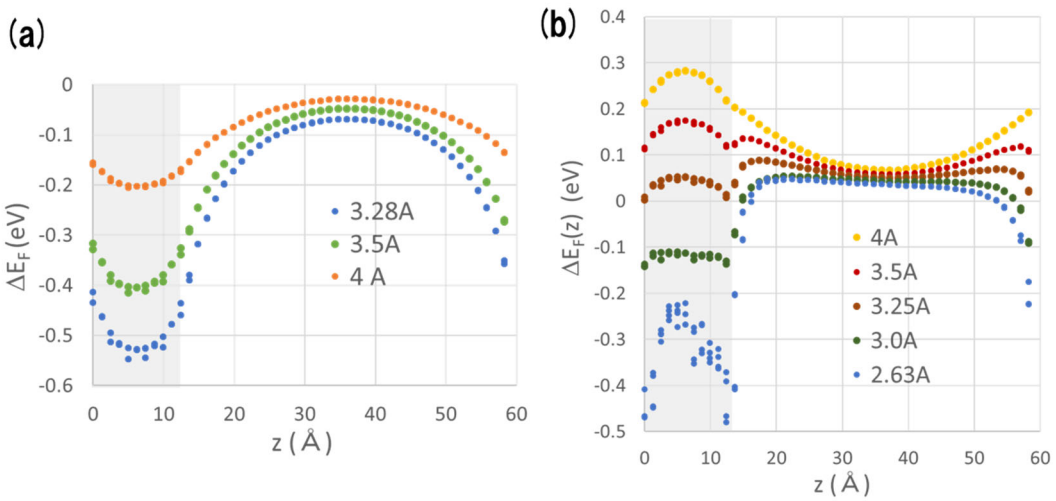
(a)
0
-0.1
-0.2
-0.3
-0.4
-0.5
-0.6
ΔE_F (eV)
0
10
20
30
40
50
60
z (Å)
3.28A
3.5A
4 A
(b)
0.4
0.3
0.2
0.1
0
-0.1
-0.2
-0.3
-0.4
-0.5
ΔE_F(z) (eV)
0
10
20
30
40
50
60
z (Å)
4A
3.5A
3.25A
3.0A
2.63A

Figure 5

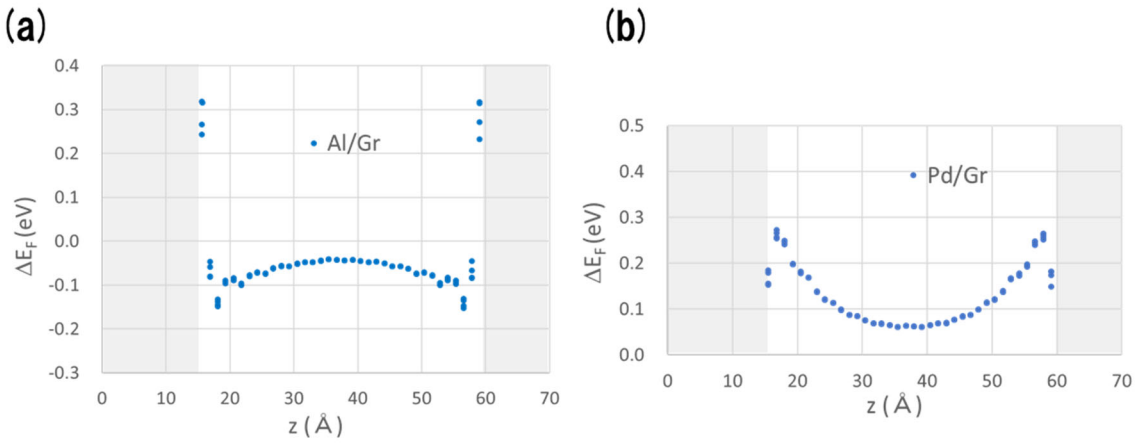
(a)
0.4
0.3
0.2
0.1
0.0
-0.1
-0.2
-0.3
ΔE_F (eV)
Al/Gr
0
10
20
30
40
50
60
70
z (Å)
(b)
0.5
0.4
0.3
0.2
0.1
0.0
ΔE_F (eV)
Pd/Gr
0
10
20
30
40
50
60
70
z (Å)

Figure 6

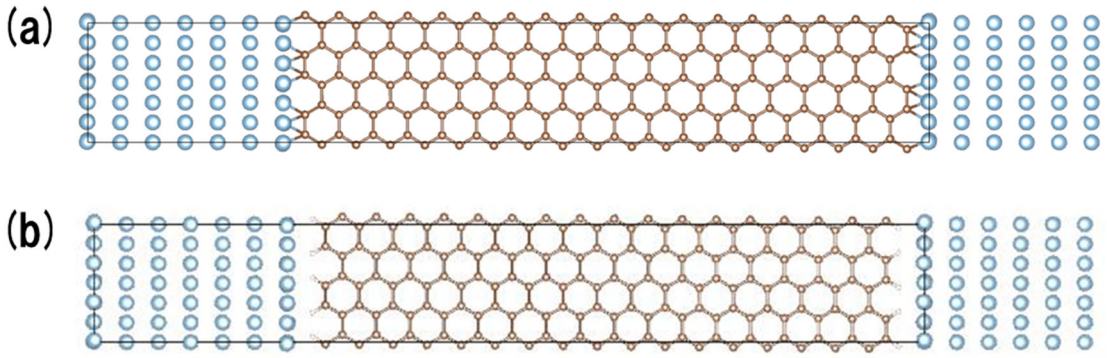

Figure 7

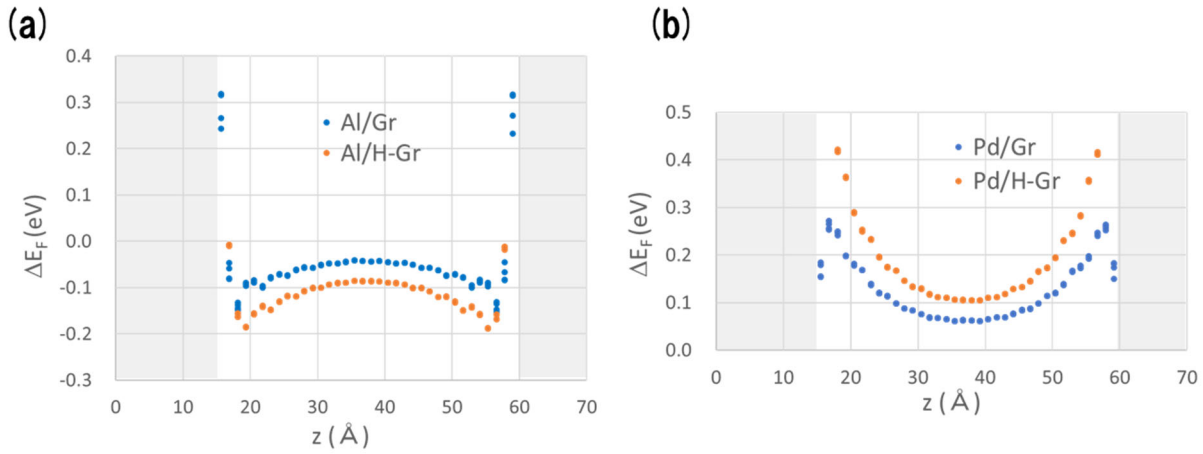
(a)
0.4
0.3
0.2
0.1
0.0
-0.1
-0.2
-0.3
ΔE_F (eV)
Al/Gr
Al/H-Gr
0
10
20
30
40
50
60
70
z (Å)
(b)
0.5
0.4
0.3
0.2
0.1
0.0
ΔE_F (eV)
Pd/Gr
Pd/H-Gr
0
10
20
30
40
50
60
70
z (Å)

Figure 8

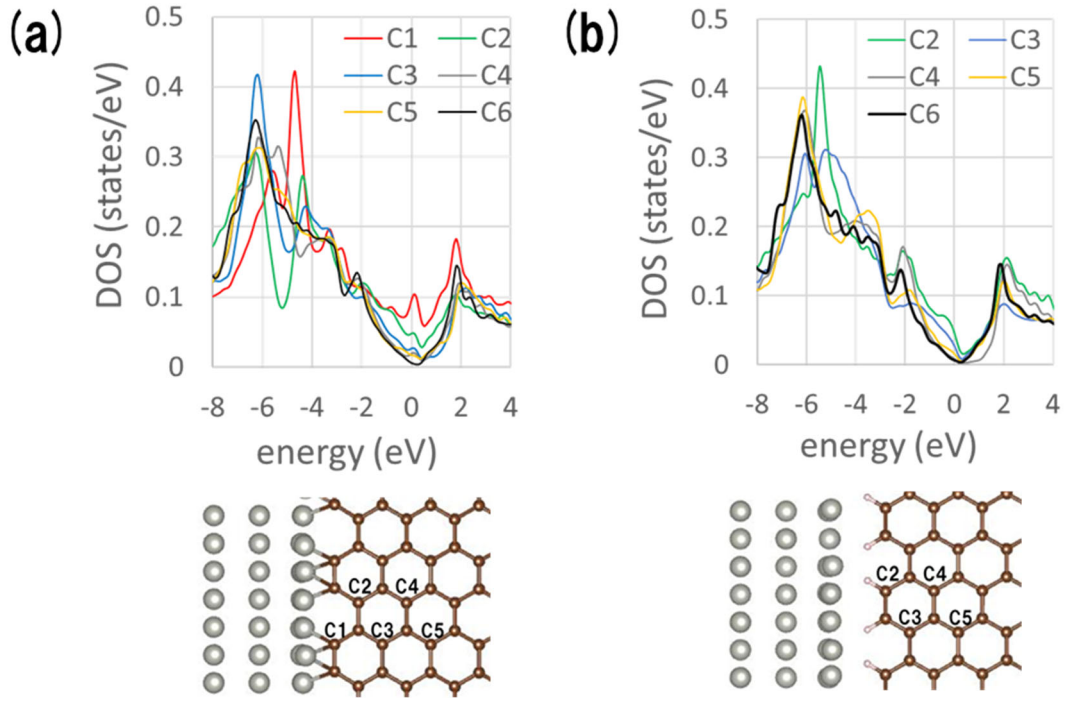
(a)
DOS (states/eV)
0.5
0.4
0.3
0.2
0.1
0
C1
C2
C3
C4
C5
C6
-8 -6 -4 -2 0 2 4
energy (eV)
C2 C4
C1 C3 C5
(b)
DOS (states/eV)
0.5
0.4
0.3
0.2
0.1
0
C2
C3
C4
C5
C6
-8 -6 -4 -2 0 2 4
energy (eV)
C2 C4
C3 C5

Figure 9